# Adaptive Estimation of the Pennes' Bio-Heat Equation - I: Observer Design

A. Cristofaro$^\star$, G. Cappellini$^\star$, E. Staffetti$^\dagger$, G. Trappolini$^\star$, M. Vendittelli$^\star$

*Abstract*— In this paper, we propose a multiple-model adaptive estimation setup for a class of uncertain parabolic reaction-diffusion PDEs encompassing the Pennes' bio-heat equation, which is a motivating case study from the perspective of biomedical applications such as hyperthermia. The efficacy of the approach in estimating the system solution and recovering the value of the reaction coefficient is validated through numerical simulations in MATLAB. The validation step has highlited some limitations of classical numerical simulation tools that we propose to handle through an implementation of the estimator relying on Deep Learning libraries. This alternative approach is reported in a companion paper (Part II of this work).

## I. INTRODUCTION

The process of heat transfer in organic tissues is described by a parabolic partial differential equation, referred to as Pennes' bio-heat equation, which is essentially a standard heat equation plus a linear reaction term. Handling properly such equation is instrumental to improving the effectiveness of minimally invasive thermal therapies [1] like, e.g., superficial hyperthermia, a treatment critically related to the actual temperature rise at the target [2], [3]. On the other hand, control and estimation for the bio-heat equation are somewhat difficult due to the presence of uncertain coefficients and to the fact that, typically, in order to avoid the use of invasive temperature sensors, one can rely on boundary measurements only.

Parabolic PDEs with parametric uncertainties have been moderately investigated in the literature. Many of the available results pertain either robust control design (see for example [4], [5], [6], [7] and the references therein) or robust/adaptive observer design with distributed measurements or structured uncertainties [8], [9], [10]. An interesting approach based on interval observers is proposed in [11]. Nevertheless, for a parabolic reaction-diffusion equation with unknown coefficient of the reaction term like the one considered in this paper, the only viable approach to adaptive estimation, among the existing ones, seems to be backstepping observer design [12], [13]. On the other hand, the synthesis of backstepping observers is based on complex integral transformations, which may prevent the method from being efficiently applied in real-time. For this reason, we investigate here a different setup based on multiple-model (MM) adaptive estimation, mimicking the approach described in [14] for finite-dimensional linear systems. This allows a

fairly accurate estimation of the solution to be obtained, which depends on the number of models considered, along with a recovery of the uncertain coefficient. In particular, the contribution of the paper is twofold. On the one hand, we investigate the design of the multiple-model adaptive observer for the general class of 1D parabolic reaction-diffusion equations. In fact, to the best of our knowledge, this is the first time that multiple models are used to tackle an adaptive estimation problem in infinite-dimensional systems. On the other hand, we use this machinery to solve the robust estimation problem for the 1D Pennes' bio-heat Equation with boundary measurements. It must be pointed out, however, that the implementation of the multiple-model scheme for a PDE seems to have some intrinsic limitations due to the reduced computational capabilities of standard solvers. To overcome such issues, the implementation of the estimation setup using PINNs is proposed in the companion paper [15], which aims at illustrating an efficient architecture for real-time applications. These results lay the basis for feedback control of temperature at the target volume in superficial hyperthermia treatments.

### A. Notation

Given a function $f : \mathbb{R}^n \to \mathbb{R}$, we denote by $\partial_{z_i} f$ the partial derivative of $f(z_1, ..., z_n)$ with respect to the variable $z_i$, $i = 1, ..., n$. The notation $L^2[0, 1]$ stands for the space of functions $f : [0, 1] \to \mathbb{R}$ whose squared integral is finite and corresponds to the $L^2$-norm, that is

$$\|f\|_{L^2} := \left( \int_0^1 |f(z)|^2 dz \right)^{\frac{1}{2}} < +\infty$$

### B. 1D Pennes' bio-heat Equation

The Pennes' bio-heat Equation describes the evolution of the temperature $T(x, t)$ in a biological tissue, and it is given by the parabolic reaction-diffusion PDE

$$\varrho c \partial_t T = \kappa_{\text{eff}} \partial_{xx} T - \varrho_b w_b c_b (T - T_a) + \mathcal{Q} \quad (1)$$

where $\varrho$ is the tissue density, $c$ is specific heat of the tissue, $k_{\text{eff}}$ is the termal conductivity of the tissue, $\varrho$ is blood density, $w_b$ is the blood perfusion rate, $c_b$ is the specific heat of blood, $T_a$ is the arterial blood temperature and $\mathcal{Q}$ is an internal heat source. The blood perfusion rate $w_b$ is bounded within a certain range, but the actual value is typically not known.

*Remark 1.1: Let us observe that, thanks to linearity, the dependency on the constant $T_a$ can always be removed from equation* (1) *by defining the change of variables $\bar{T} := T - T_a$.*

## II. PROBLEM FORMULATION AND PROPOSED APPROACH

In light of Remark 1.1 and upon appropriate transformations, detailed in [15] and inspired by [16], the 1D bio-heat Equation (1) can be recast as a linear reaction-diffusion

equation in the general form

$$\partial_t T = \sigma \partial_{xx} T - \omega T + \Psi \tag{2}$$

defined for $(x,t) \in [0,1] \times [0,+\infty)$ with Robin-type boundary conditions

$$\begin{aligned} T(0,t) &= C_0 \quad t \geq 0 \\ \partial_x T(1,t) &= v(t) \quad t \geq 0 \end{aligned} \tag{3}$$

where $C_0 \in \mathbb{R}$ is a known constant and $v(t)$ is a boundary input, and with initial condition

$$T(x,0) = T_0(x) \quad x \in [0,1] \tag{4}$$

The coefficient $\sigma > 0$ is a known positive constant, the coefficient $\omega \geq 0$ is possibly unknown and $\Psi = \Psi(x,\cdot) \in C([0,+\infty); L^2(0,1))$ is a known smooth internal source. The boundary conditions (3) describe a setup characterized by a fixed temperature at one side of the domain and a tunable heat flux at the other side. In particular, referring to the inspiring model (1) presented earlier, the boundary $x = 0$ corresponds to the deepest point in the tissue, whereas $x = 1$ corresponds to the skin surface.

Let us assume that the value of the input $v(t)$ is accessible and that, in addition, the output

$$y(t) = T(1,t) \tag{5}$$

is available at any $t \geq 0$. The initial condition $T_0(x)$ and the input $v(t)$ are supposed to be smooth enough to guarantee the existence of a mild solution [17]. Let us give the following assumption which will be used in the formulation of later results.

*Assumption 2.1:* The non-negative coefficient $\omega$ satisfies:
   i) $\omega$ is constant;
   ii) there exist known lower and upper bound $\omega_{\min}, \omega_{\max}$ with $0 \leq \omega_{\min} \leq \omega \leq \omega_{\max}$.

Bearing this in mind, the main goal is to reconstruct asymptotically the solution $T(x,t)$ to the PDE (2) with boundary/initial conditions (3)-(4) using only measurements of $y(t)$ and knowledge of $v(t)$ and $\Psi(x,t)$.

### A. Observer structure

Let us preliminarily address the observer design problem for the case of $\omega$ fulfilling Assumption 2.1 and known. To construct an observer $\hat{T}(x,t)$, consider first a copy of the PDE dynamics (2)

$$\partial_t \hat{T} = \sigma \partial_{xx} \hat{T} - \omega \hat{T} + \Psi \tag{6}$$

defined for $(x,t) \in [0,1] \times [0,+\infty)$ with boundary conditions

$$\begin{aligned} \hat{T}(0,t) &= C_0 \\ \partial_x \hat{T}(1,t) &= v(t) + \alpha(y(t) - \hat{T}(1,t)) \end{aligned} \tag{7}$$

where $\alpha > 0$ is the output injection gain. The compatibility conditions for the initialization of the observer $\hat{T}_0(x)$ read then as

$$\hat{T}_0(0) = T_0(0) \ \wedge \ \partial_x \hat{T}_0(x)|_{x=1} + \alpha \hat{T}_0(1) = v(0) + \alpha T_0(1)$$

Setting $e_T(x,t) := T(x,t) - \hat{T}(x,t)$ and $e_{T,0}(x) := e_T(x,0)$, the error dynamics is governed by the PDE

$$\begin{aligned} \partial_t e_T &= \sigma \partial_{xx} e_T - \omega e_T \\ e_T(0,t) &= 0 \\ \partial_x e_T(1,t) &= -\alpha e_T(1,t) \end{aligned} \tag{8}$$

*Remark 2.1:* The well-posedness of the above error dynamics follows immediately from classical semigroup theory arguments [17].

Next result addresses observer convergence in nominal conditions, i.e. under the assumption that $\omega$ is constant and known.

*Proposition 2.1:* Assume that $\hat{T}_0(x)$ is smooth, and consider the observer dynamics (6)-(7). For any $\alpha > 0$, the $L^2$-norm of the error

$$\|T(\cdot,t) - \hat{T}(\cdot,t)\|_{L^2}$$

*converges exponentially to zero, with a decay rate not smaller than* $\min\{\sigma\alpha, \sigma\pi^2/4\} + \omega$.

**Proof.** Consider the Lyapunov functional candidate

$$V(t) = \frac{1}{2} \int_0^1 e_T^2 \, dx$$

corresponding to $\frac{1}{2}\|e_T\|_{L^2}^2$. We aim at diffentiating $V(t)$ along the error system solutions and, as the latter are mild solutions thanks to the smoothness of initial and boundary conditions, one is allowed to bring the derivative under the integral sign, so that

$$\dot{V}(t) = \int_0^1 e_T \partial_t e_T \, dx = \sigma \int_0^1 e_T \partial_{xx} e_T \, dx - \omega \int_0^1 e_T^2 \, dx$$

where the equation of the error system has been used. Let us focus on the first term in the right-hand side. Performing integration by parts and using the boundary conditions, one has

$$\begin{aligned} \int_0^1 e_T \partial_{xx} e_T \, dx &= e_T \partial_x e_T \Big|_0^1 - \int_0^1 (\partial_x e_T)^2 \, dx \\ &= e_T(1,t) \partial_x e_T(1,t) - \underbrace{e_T(0,t) \partial_x e_T(0,t)}_{=0} \\ &\quad - \int_0^1 (\partial_x e_T)^2 \, dx \\ &= -\alpha(\partial_x e_T(1,t))^2 - \int_0^1 (\partial_x e_T)^2 \, dx \end{aligned}$$

Now, recalling Poincaré-Wirtinger inequality [18, Remark 2.2], we have that

$$-\alpha(\partial_x e_T(1,t))^2 - \int_0^1 (\partial_x e_T)^2 \, dx \leq -\eta \int_0^1 e_T^2 \, dx$$

with

$$\eta = \eta(\alpha) = \begin{cases} \alpha & \alpha \in \left(0, \dfrac{\pi^2}{4}\right) \\ \dfrac{\pi^2}{4} & \alpha \geq \dfrac{\pi^2}{4} \end{cases}$$

Summarizing, we have shown that

$$\dot{V}(t) \leq -(\sigma\eta + \omega) \int_0^1 e_T^2 \, dx = -2(\sigma\eta + \omega)V(t)$$

thus yielding exponential convergence of $V(t)$ with a decay rate not smaller than $2(\sigma\eta + \omega) = 2(\min\{\sigma\alpha, \sigma\pi^2/4\} + \omega)$. The statement then follows by the simple observation that the norm $\|e_T\|_{L^2}$ satisfies the identity $\|e_T\|_{L^2} = \sqrt{2}V(t)^{\frac{1}{2}}$. ♣

*B. Sensitivity analysis*

The previous result proves observer convergence in nominal conditions. Next we will investigate the sensitivity of the error with respect to uncertainty in the coefficient $\omega$. To this end, consider a claimed value $\tilde{\omega}$ to be used in the observer state equation, which becomes

$$\partial_t\hat{T} = \sigma\partial_{xx}\hat{T} - \tilde{\omega}\hat{T} + \Psi \qquad (9)$$

with boundary conditions left unchanged. Considering again the Lyapunov functional $V(t)$ for the error $e_T(x,t)$ and following the same steps of the proof of Proposition 2.1, we end up with the inequality

$$\dot{V}(t) \leq -2\sigma\eta V(t) - \omega\int_0^1 Te_T dx + \tilde{\omega}\int_0^1 \hat{T}e_T dx$$

Now, adding and subtracting the same quantity $\tilde{\omega}\int_0^1 Te_T dx$ and using Young's inequality, the latter can be rewritten as

$$\begin{aligned}
\dot{V}(t) &\leq -2\sigma\eta V(t) - \tilde{\omega}\int_0^1 e_T^2 dx + (\tilde{\omega}-\omega)\int_0^1 Te_T dx \\
&= -2(\sigma\eta + \tilde{\omega})V(t) + (\tilde{\omega}-\omega)\int_0^1 Te_T dx \\
&\leq -2(\sigma\eta + \tilde{\omega})V(t) \\
&\quad + \frac{|\tilde{\omega}-\omega|}{2}\left(\frac{1}{\delta}\int_0^1 T^2 dx + \delta\int_0^1 e_T^2 dx\right) \\
&= -(2\sigma\eta + 2\tilde{\omega} - \delta|\tilde{\omega}-\omega|)V(t) + \frac{|\tilde{\omega}-\omega|}{2\delta}\int_0^1 T^2 dx
\end{aligned}$$

where $\delta > 0$ is an arbitrary positive scalar. Notice that, however, in order to keep the coefficient in first term on the right-hand side negative, we must impose the upper bound $\delta < 2(\sigma\eta + \tilde{\omega})/|\tilde{\omega}-\omega|$. Based on the previous computations, we can give the following corollary addressing the observer sensitivity.

*Corollary 2.1:* Let $\omega > 0$ be unknown, and consider the observer (9) with some guess $\tilde{\omega} > 0$. Assume that a constant $T_{\max} > 0$ exists such that the bound $T(x,t) \leq T_{\max}$ holds for any $x \in [0,1]$ and any $t \geq 0$. Then the error $e_T(x,t)$ is ultimately bounded relative to the set

$$\mathcal{E} := \{e_T \in L^2(0,1) : \|e_T\|_{L^2}^2 \leq 4c_0\}$$

where $c_0 = \dfrac{|\tilde{\omega}-\omega|^2 T_{\max}^2}{(\sigma\eta + \tilde{\omega})^2}$. Furthermore, the convergence towards the attractive set $\mathcal{E}$ is exponential, with a rate not smaller than $(\sigma\eta + \tilde{\omega})/2$.

**Proof.** From earlier derivations, using the upper bound on $T(x,t)$ and further rearranging terms, we have

$$\begin{aligned}
\dot{V}(t) &\leq -(2\sigma\eta + 2\tilde{\omega} - \delta|\tilde{\omega}-\omega|)V(t) + \frac{|\tilde{\omega}-\omega|}{2\delta}\int_0^1 T^2 dx \\
&\leq -(\sigma\eta + \tilde{\omega})V(t) \\
&\quad - \left((\sigma\eta + \tilde{\omega} - \delta|\tilde{\omega}-\omega|)V(t) - \frac{|\tilde{\omega}-\omega|}{2\delta}T_{\max}^2\right)
\end{aligned}$$

The quantity in the brackets is non-negative whenever

$$V(t) \geq \frac{|\tilde{\omega}-\omega|T_{\max}^2}{2\delta(\sigma\eta + \tilde{\omega} - \delta|\tilde{\omega}-\omega|)}$$

and, minimizing with respect to the positive parameter $\delta$, one gets the sharper condition

$$V(t) = \frac{1}{2}\|e_T(\cdot,t)\|_{L_2}^2 \geq 2c_0$$

which in turn implies that

$$\dot{V}(t) \leq -(\sigma\eta + \tilde{\omega})V(t) \quad \forall e_T(\cdot,t) \in \mathcal{E}^c := L^2(0,1)\setminus\mathcal{E}$$

The latter inequality guarantees global attractivity of the bounded set $\mathcal{E}$, with the claimed rate of exponential convergence. ♣

## III. MULTIPLE-MODEL ADAPTIVE SCHEME

The sensitivity analysis of the previous section suggests to devise a method for reducing the uncertainty on the perfusion coefficient $\omega$ so as to get better estimation results. Standard adaptive control strategies, based on LaSalle's invariance principle, are not applicable in this case, due to the nonlinearity appearing in the evaluation of the Lyapunov function derivative, which depends on both the unknown parameter $\omega$ and the full state $T$. Available approaches based on backstepping can be used [12], but these come at the price of introducing quite complex coordinate transformations.

In this work, we pursue an alternative way that hinges on multiple-models [19], [20], which are well suited here because, in light of Assumption 2.1, the unknown parameter belongs to a bounded admissible range. Bearing this in mind, let us consider a set of fixed values $\omega_j \geq 0$, $j = 1, ..., N$ for some $N \in \mathbb{N}$, with

$$\omega_1 < \omega_2 < \cdots < \omega_N$$
$$\omega_1 \leq \omega_{\min}, \quad \omega_{\max} \leq \omega_N$$

Accordingly, let us define a family of observers $\hat{T}^{(j)}(x,t)$ with the structure (9) and with the choice $\tilde{\omega} = \omega_j$, that is

$$\begin{aligned}
\partial_t\hat{T}^{(j)} &= \sigma\partial_{xx}\hat{T}^{(j)} - \omega_j\hat{T}^{(j)} + Q \\
\hat{T}^{(j)}(0,t) &= 0 \\
\partial_x\hat{T}^{(j)}(1,t) &= v(t) + \alpha(y(t) - \hat{T}^{(j)}(1,t))
\end{aligned}$$

It is worth noticing that, for each observer within this family, an ultimate bound for the corresponding estimation error is provided by Corollary 2.1. Following the approach proposed in [14], the idea is then to introduce an overall estimator

$$\hat{T}^\dagger(x,t) = p_1(t)T^{(1)}(x,t) + \cdots + p_N(t)T^{(N)}(x,t) \quad (10)$$

obtained as dynamic convex combination of the observers $T^{(j)}(x,t)$ with weights $p_j(t)$ being updated according to

$$\dot{p}_j(t) = -\lambda\left(1 - \frac{e^{-\mu_j(t)}}{\sum_{\ell=1}^N p_\ell(t)e^{-\mu_\ell(t)}}\right)p_j(t) \quad j = 1, ..., N$$
$$(11)$$

where $\mu_j(t) := v|T(1,t) - \hat{T}^{(j)}(1,t)|^2$, $v > 0$, is the (absolute) output error and $\lambda > 0$ is the adaptive gain.

The overall observer (10) corresponds to a weighted average of the individual observers, whose weights adapt based on

the size of the associated output errors. Whenever one of these errors is ultimately smaller than the others, with

$$\lim_{t \to +\infty} \sup \; (\mu_j^\star(t) - \mu_\ell(t)) < 0 \quad \forall \ell \neq j^\star,$$

one may expect the convergence of the weights to the values

$$\lim_{t \to \infty} p_{j^\star}(t) = 1, \quad \lim_{t \to \infty} p_\ell(t) = 0 \quad \forall \ell \neq j^\star,$$

so that (10) reduces to $\hat{T}^\dagger(x,t) = p_{j^\star}(t)T^{(j^\star)}(x,t)$ (see [14, Theorem 1]). This means that $\hat{T}^{(j^\star)}(x,t)$ results being the *best* observer among the considered family $\{\hat{T}^{(j)}(x,t)\}_{j=1,...,N}$, with respect to the inherent output error function.

*Remark 3.1:* Invoking again Corollary 2.1, we can notice that the finer the gridding of $[\omega_{\min}, \omega_{\max}]$ is (or, equivalently, the larger the number of models $N$ is), the smaller the ultimate set $\mathcal{E}$ associated to the best observer $\hat{T}^{(j)}$ gets.

## IV. SIMULATIONS

### A. Implementation

All simulation results in this paper have been obtained in MATLAB using the `pdepe` built-in routine. Although the solver is quite efficient at handling simple systems of PDEs, it is not suited for encoding systems of PDEs (bio-heat Equations, observers) and ODEs (dynamic weights). In our companion paper [15] we propose an implementation scheme based on neural networks. We consider here an alternative and naive approach, consisting in treating the dynamics of weights as a degenerate PDE, *i.e.*, with uniform spatial dependency, which allows them to be embedded in the system of PDEs. Despite the benefits of a simpler implementation, this method suffers however from some numerical issues that will be discussed further on, thus indicating the learning-based procedure proposed in [15] as the most promising and suitable for real-time applications.

*Artificial PDE formulation for the weights:* The weights $p_j(t)$ are naturally governed by the ordinary differential equations (11). However, it can be observed that, when using a built-in PDE solver such as `pdepe` in MATLAB, one may encounter some issues with getting in real time the output feedback from the PDEs' solutions needed to implement the ODEs. To overcome the problem, one may use a partial differential version of (11), obtained by introducing an artificial dependency on the spatial variable, and which delivers equivalent solutions. This can be done, for example, by defining $p_j(x,t)$, $j = 1,...,N$, as the solutions to the following system of nonlinear parabolic PDEs with homogenous Neumann conditions

$$\partial_t p_j(x,t) = \gamma \partial_{xx} p_j(x,t)$$

$$- \lambda \left(1 - \frac{e^{-\mu_j(t)}}{\sum_{\ell=1}^{N} p_\ell(x,t)e^{-\mu_\ell(t)}}\right) p_j(x,t)$$

$$\partial_x p_j(0,t) = \partial_x p_j(1,t) = 0$$

where $\gamma > 0$ and initialization $p_j(x,0)$ are independent of the spatial variable $x$ for any $j = 1,...,N$.

### B. Results

Consider the bio-heat Equation (1) for a muscular tissue without an internal source, *i.e.* setting $\mathcal{Q} \equiv 0$, with coefficients taken accordingly to [21], as reported in Table I.

TABLE I: Parameters of the bio-heat Equation

| Parameter | $\varrho$, $\varrho_b$ | $c$, $c_b$ | $\kappa_{\text{eff}}$ | $T_a$ |
|---|---|---|---|---|
| Value | 1050, 1043 | 3639, 3825 | 5 | 37 |
| Unit | $[kg/m^3]$ | $[J/(kg \cdot K)]$ | $[W/(m \cdot K)]$ | $^\circ C$ |

The blood perfusion rate is $w_b = 2.22 \cdot 10^{-3} \; [s^{-1}]$, with an admissible range $[w_{\min}, w_{\max}] = [0.43 \cdot 10^{-4}, 3.8 \cdot 10^{-3}]$. A spatial rescaling has been applied so that the length of the interval $[0,1]$ corresponds to $5\,cm$, whereas the simulation time interval has been restricted to $[0, t_f]$ with $t_f = 1800\,s$. Initial and boundary conditions have been chosen as follows:

$$T(x,0) = T_a + q_0 \frac{x^4}{4} + \beta x(x-1)^2 \quad \forall x \in [0,1]$$
$$T(t,0) = T_a \quad \forall t \geq 0$$
$$\partial_x T(t,1) = q_0 \quad \forall t \geq 0$$

with $q_0 = 16$ and $\beta = 15$. Notice that the equation can be brought into the model form (2) by setting

$$\sigma := \frac{d^2 \kappa_{\text{eff}}}{\varrho c}, \quad \omega := \frac{\varrho_b w_b c_b}{\varrho c}$$

where $d = 20$ is the rescaling factor, and applying a change of coordinates as sketched in Remark 1.1. The numerical solution of the equation is depicted in Figure 1.

*Example 4.1:* We begin the illustration of the results on observer design by considering the case of known perfusion rate $w_b$. Following the construction given in Section II-A, we consider an observer in the form (6), with output injection gain $\alpha = 30$ and initial condition

$$\hat{T}(x,0) = T_a + q_0 \frac{x^4}{4} \tag{12}$$

As expected, the observer $\hat{T}(x,t)$ successfully achieves the reconstruction of the temperature $T(x,t)$ over the whole domain $[0,1]$. The temperature profile along with the estimated



Numerical solution of the system computed with 100 mesh points.

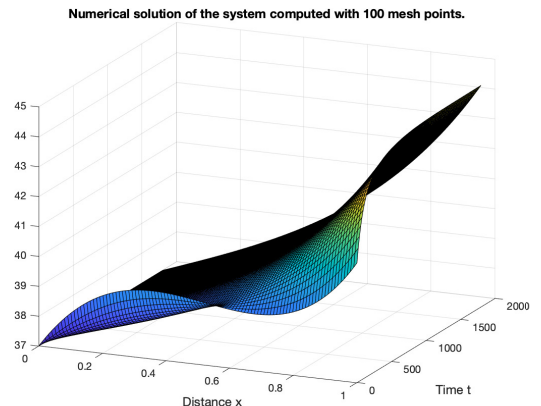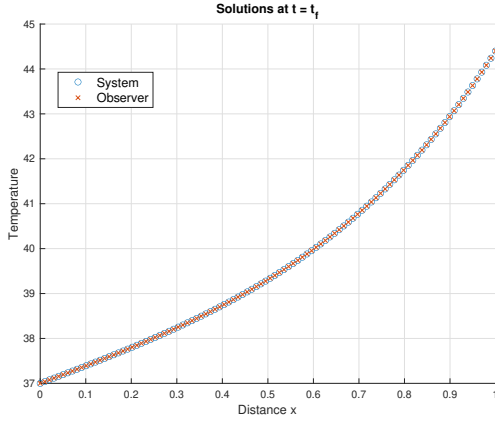Fig. 1: Numerical solution of the bio-heat Equation

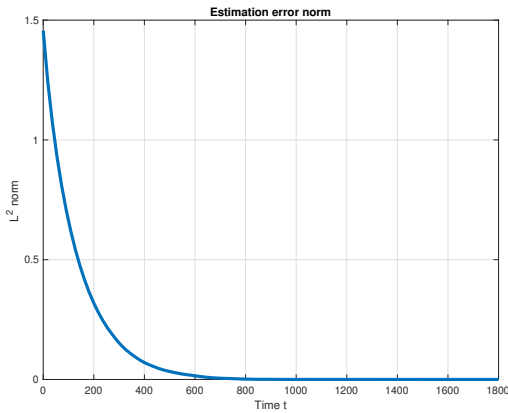Fig. 2: Example 1: System vs. observer at $t = t_f$



Fig. 3: Example 1: $L^2$-norm of the estimation error

temperature profile at the final time $t_f = 1800\,s$ are shown in Figure 2, while Figure 3 shows the exponential decay of the $L^2$-norm of the estimation error $T(x, t) - \hat{T}(x, t)$.

*Example 4.2:* Let us now assume that $w_b$ is unknown, and consider the multiple-model approach proposed in Section III with $N = 8$ models computed based on a uniform gridding $\{w_1, w_2, \ldots, w_8\}$ of the range $[w_{\min}, w_{\max}]$, so that the closest value to the actual perfusion rate is $w_5$. Each model $\hat{T}^j(x, t)$, $j = 1, 2, \ldots, 8$, has been initialized as in (12) and implemented using the artificial PDE formulation for the dynamics of the weights $p_j$ described in Section IV-A with parameters

$$\gamma = 10, \quad \lambda = 200, \quad \upsilon = 500$$

In this case, for computational reasons (see also the following Remark 4.1), it has been necessary to increase the output injection gain in the observers up to $\alpha = 3 \cdot 10^4$. Based on the dynamic weights $p_j(x, t)$, we have evaluated the multiple-model adaptive observer $\hat{T}^\dagger(x, t)$ defined as in (10). The comparison of system solution $T(x, t)$, observers $\hat{T}^{(j)}(x, t)$ and MM adaptive observer $\hat{T}^\dagger(x, t)$ at the final time $t_f = 1800\,s$ is proposed in Figure 4, and a zoomed version for helping visualization of results is given in Figure 5. While the system and the observers coincide at the

boundary points, deviations arise inside the domain due to the wrongly guessed values of $w_b$. However, as clearly visible in Fig. 5, the observer $\hat{T}^{(4)}(x, t)$ is close to the actual system, which is indeed quite accurately reconstructed by the MM adaptive observer $\hat{T}^\dagger(x, t)$. The latter is built according to the dynamic weights $p^j(x, t)$, whose time evolution is reported in Figure 6. Despite a steady-state condition is not reached, one can see that the largest weights are those corresponding to the values $w_4$ and $w_5$ lying "around" the actual value $w_b$, thus confirming that a correct estimation of the perfusion rate is achieved. Finally, the evolution of the $L^2$-norm of the error $T(x, t) - \hat{T}^\dagger(x, t)$ is depicted in Figure 7: after the initial descent, corresponding to the observer transient, the error norm reaches a steady-state value which is, as expected, small but not zero.

*Remark 4.1:* Due to the somewhat limited computational capabilities of the `pdepe` routine, not all the choices for system parameters were feasible. For example, as already mentioned, picking a small injection gain would make the solver incurring in numerical instabilities. For the same reason, the learning rate $\lambda$ of dynamic weights, is bounded to be sufficiently small in the current simulation setup, which results in a fairly slow adaptation. In the companion paper [15], we propose a deep learning approach for efficient implementation of the coupled PDE/ODE dynamics of the multiple-model observer. In short, a set of deep neural networks, pre-trained with different values of the perfusion rate $w_b$, implement the dynamics of the observers, which, taking the estimation error as input, are able to predict the temperature in the whole domain of interest in real-time without incurring in the above mentioned numerical issues.

## V. CONCLUSIONS

Observer design for a class of 1D parabolic linear reaction-diffusion equations has been considered, with the Pennes' bio-heat Equation as main application case. Assuming uncertainty in the reaction coefficient, a multiple-model adaptive scheme, already proven to be efficient for finite-dimensional systems, has been extended to the considered class of linear 1D PDEs with boundary outputs, with the aim of simultaneously estimating the system solution and recovering the
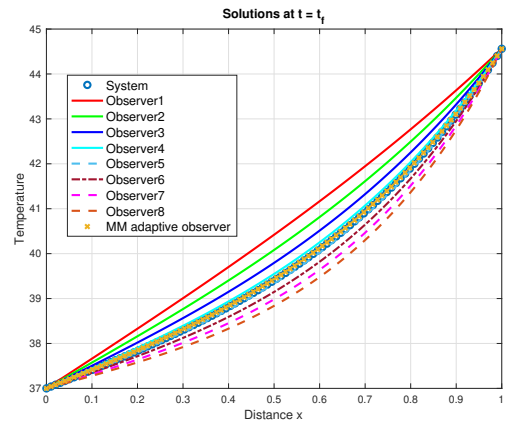


Fig. 4: Example 1: System vs. observers at $t = t_f$

uncertain parameter. The performance of the method, along with some potential implementation issues, are illustrated through MATLAB simulations. The criticalities higlited by the simulation campain led [15] to an alternative implementation relying on deep neural networks. Future work will be devoted to generalizing the observer design to higher dimensional equations, and to considering possibly time-varying uncertain coefficients, following an approach similar to the one proposed in [22].



Fig. 5: Example 2: System vs. observers at $t = t_f$ (zoom)



Fig. 6: Example 2: Dynamic weights



Fig. 7: Example 2: $L^2$-norm of the estimation error

## REFERENCES

[1] H. P. Kok, E. N. Cressman, W. Ceelen, C. L. Brace, R. Ivkov, H. Grüll, G. Ter Haar, P. Wust, and J. Crezee, "Heating technology for malignant tumors: A review," *International Journal of Hyperthermia*, vol. 37, no. 1, pp. 711–741, 2020.

[2] H. D. Trefná et al., "Quality assurance guidelines for superficial hyperthermia clinical trials: I. clinical requirements," *International Journal of Hyperthermia*, vol. 33, no. 4, pp. 471–482, 2017.

[3] A. Bakker, "Improving superficial hyperthermia treatment: Temperature matters," Ph.D. dissertation, 2021.

[4] M. Kishida and R. D. Braatz, "Structured spatial control of the reaction-diffusion equation with parametric uncertainties," in *Proc. of 2010 IEEE Int. Symposium on Computer-Aided Control System Design*, 2010, pp. 1097–1102.

[5] F. Mazenc and C. Prieur, "Strict Lyapunov functions for semilinear parabolic partial differential equations," *Mathematical Control and Related Fields*, vol. 1, no. 2, pp. 231–250, 2011.

[6] I. Karafyllis and M. Krstic, "ISS with respect to boundary disturbances for 1-D parabolic PDEs," *IEEE Transactions on Automatic Control*, vol. 61, no. 12, pp. 3712–3724, 2016.

[7] A. Cristofaro, "Robust distributed control of quasilinear reaction–diffusion equations via infinite-dimensional sliding modes," *Automatica*, vol. 104, pp. 165–172, 2019.

[8] M. A. Demetriou and I. Rosen, "Unknown input observers for a class of distributed parameter systems," in *Proceedings of the 44th IEEE Conference on Decision and Control*. IEEE, 2005, pp. 3874–3879.

[9] T. Ahmed-Ali, F. Giri, M. Krstic, F. Lamnabhi-Lagarrigue, and L. Burlion, "Adaptive observer for a class of parabolic PDEs," *IEEE Transactions on Automatic Control*, vol. 61, no. 10, pp. 3083–3090, 2015.

[10] W. Hu and M. A. Demetriou, "Observer design with sparsity for parabolic PDEs," *IFAC-PapersOnLine*, vol. 52, no. 2, pp. 180–182, 2019.

[11] T. Kharkovskaia, D. Efimov, E. Fridman, A. Polyakov, and J.-P. Richard, "On design of interval observers for parabolic PDEs," *IFAC-PapersOnLine*, vol. 50, no. 1, pp. 4045–4050, 2017.

[12] A. Smyshlyaev and M. Krstic, "Backstepping observers for a class of parabolic PDEs," *Systems & Control Letters*, vol. 54, no. 7, pp. 613–625, 2005.

[13] P. Ascencio, A. Astolfi, and T. Parisini, "An adaptive observer for a class of parabolic pdes based on a convex optimization approach for backstepping pde design," in *2016 American Control Conference (ACC)*. IEEE, 2016, pp. 3429–3434.

[14] V. Hassani, A. P. Aguiar, A. M. Pascoal, and M. Athans, "Further results on plant parameter identification using continuous-time multiple-model adaptive estimators," in *Proceedings of the 48h IEEE Conference on Decision and Control (CDC)*, 2009, pp. 7261–7266.

[15] G. Cappellini, A. Cristofaro, E. Staffetti, G. Trappolini, and M. Vendittelli, "Adaptive estimation of the Pennes' Bio-Heat equation - II: a NN-based implementation for real-time applications," in *62nd IEEE Conference on Decision and Control*, 2023.

[16] J. Okajima, S. Maruyama, H. Takeda, and A. Komiya, "Dimensionless solutions and general characteristics of bioheat transfer during thermal therapy," *Journal of Thermal Biology*, vol. 34, no. 8, pp. 377–384, 2009.

[17] R. F. Curtain and H. Zwart, *An introduction to infinite-dimensional linear systems theory*. Springer Science & Business Media, 2012, vol. 21.

[18] M. Krstic and A. Smyshlyaev, "Adaptive control of PDEs," *Ann. Rev. Control*, vol. 32, pp. 149–160, 2008.

[19] S. N. Sheldon and P. S. Maybeck, "An optimizing design strategy for multiple model adaptive estimation and control," in *29th IEEE Conference on Decision and Control*. IEEE, 1990, pp. 3522–3527.

[20] R. Murray-Smith and T. A. Johansen, *Multiple model approaches to nonlinear modelling and control*. CRC press, 2020.

[21] M. L. V. D. Gaag, M. D. Bruijne, T. Samaras, J. V. D. Zee, and G. C. V. Rhoon, "Development of a guideline for the water bolus temperature in superficial hyperthermia," *International Journal of Hyperthermia*, vol. 22(8), pp. 637–656, 2006.

[22] A. Cristofaro, T. A. Johansen, and A. P. Aguiar, "Icing detection and identification for unmanned aerial vehicles: Multiple model adaptive estimation," in *2015 European Control Co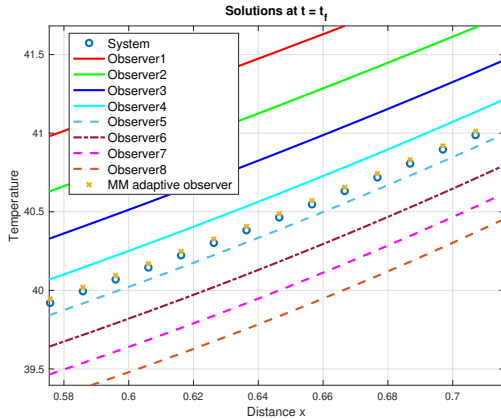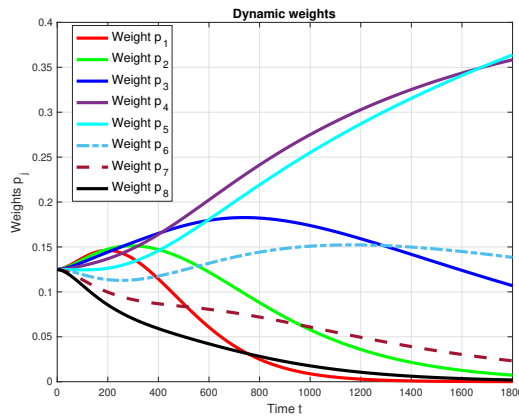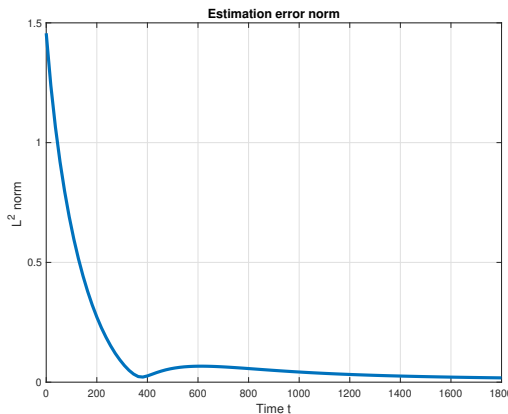nference (ECC)*. IEEE, 2015, pp. 1651–1656.